

A Possible Rotation in Al-Buqeia Rocks of Western Syria as a Result of the Left-lateral Movement of the Dead Sea Fault system.

Jamal Abou-Deeb

Geology Department, Faculty of Science, Damascus University, Syria

Received 17/03/2009

Accepted 03/11/2009

ABSTRACT

Palaeomagnetism of 75 sites from the Upper Pliocene basaltic rocks of Al-Buqeia, west of Homs, were studied. They are mostly within 5 km of both flanks of the Northern Dead Sea Fault system, and show consistent directions of magnetic remanence in most sites. Normal, Reversed and Intermediate polarities are identified, with Reversed polarities dominating. When the mean directions of the Normal sites are reversed, all sites gave similar mean inclination values, 48.2° ($\delta\text{Inc.} = 2.7^\circ$), but the site mean declinations show a regional pattern. Sites from the 3 regions west of the Fault zone (Marmarita, Qalat El-Hossen, Tel Kalakh) have similar declinations, 186° ($\delta\text{Dec.} = 5.4^\circ$). These are consistent with those from Sufer and East Ain-Kut regions, 197° ($\delta\text{Dec.} = 3.9^\circ$), furthest east of the Fault zone. All these localities have directions that are consistent with those expected for this part of Arabia in the Upper Pliocene. However, all sites east and close to the Fault zone (Bahur, West Ain-Kut, Mzeineh and Al-Buqeia) have more eastern declinations, averaging $154.0 \pm 12.0^\circ$. The declination difference, 37.3° , indicates the presence of rotated blocks adjacent to the eastern side of the Northern Dead Sea Fault system. If such a rotation took place, then a possible crustal shortening took place which is consistent with the 25 km displacement predicted for this location and appears consistent with the subsequent tectonic evolution of the Northern Dead Sea Fault system during the last 5 Ma.

Key words: Palaeomagnetism, Northern Dead Sea Fault system, Upper Pliocene, Buqeia, Missyaf and Ghab.

2009/03/17
2009/11/03

75
()
5
($\delta\text{Inc.} = 2.7^\circ$) 48.2°
()
($\delta\text{Dec.} = 5.4^\circ$) 186°
($\delta\text{Dec.} = 3.9^\circ$) 197°
)
37.3° .154° ±12.0° (
25
:

Introduction and Regional Geology

The Dead Sea Fault system (DSFS), striking north-south, and extends nearly 1000 km from the Gulf of Aqaba in the south to join the East Anatolian Fault zone in southern Turkey. It is a sinistral transform boundary separating Arabia from Africa. Due to its importance as an active major plate boundary, that may help in a better understanding of the nature, tectonic evolution and earthquake hazard of the area, and being one of the largest strike-slip fault system in the world, it became the focus of many studies (Dubertret, 1970; Freund *et al.*, 1970; Ben-Menahem *et al.*, 1976; Garfunkel *et al.*, 1981; Kellogg and Rynolds, 1983; Quennell, 1984; Ron, 1987; Hempton, 1987; Walley, 1988; Ambraseys and Barazangi, 1989; Girdler, 1990; Menzies *et al.*, 1990; Chaimov *et al.*, 1990; Trifonov *et al.*, 1991; Khair *et al.*, 1993; Sigachev *et al.*, 1995; Butler *et al.*, 1997; Beydoun, 1999; Brew *et al.*, 2001; Gomez *et al.*, 2003; Meghraoui *et al.*, 2003; Chorowicz *et al.*, 2005; Gomez *et al.*, 2006 and Gomez *et al.*, 2007).

The total strike-slip offset between Arabia and Africa in the southern part of the DSFS is established to be about 105 km (Quennell, 1984) and the present-day relative motion between the two plates is between 4-8 mm/year (Joffe and Garfunkel, 1987; Jestin *et al.*, 1994). Two strike-slip motion episodes are suggested, that is Miocene slip of 60 to 65 km and post-Miocene slip of 40 to 45 km (Freund *et al.*, 1970; Quennell, 1984). The post-Miocene slip in the northern fault segment includes 20 km suggested by Chemov *et al.*, (1990) to be consumed in shortening in the Palmyride folding.

The Northern Dead Sea transform fault system (Ponikarov, 1966; Best *et al.*, 1993) – is the northern-most extension of the Dead Sea transform fault system (Dubertret, 1970, Girdler, 1990) enters Syria from northern Lebanon, where it is called the Yemmunah Fault (eastern branch) and the Roum Fault (western Branch), and, in Syria, forms the Missyaf-Ghab fault system. That zone widens in the north to form the rhomb-shaped Missyaf-Ghab graben (Sigachev *et al.*, 1995). The Yemmunah and Missyaf-Ghab fault systems are together widely regarded as the major seismic zone and the source of the volcanic activity in the area with a predicted left lateral displacement of about 20-25 km (Quennell, 1984; Trifonov *et al.*, 1991). Although Butler *et al.*, (1997) concluded that neither of these zones had been active during the past 5 Ma but that; during this time, seismic activity had mostly been associated with the Roum Fault that extends from south Lebanon through Beirut (Butler *et al.*, 1997). Recent palaeoseismic studies on Serghaya and Missyaf segments of the

Northern Dead Sea Fault, Meghraoui et al. (2003), Gomez et al. (2003), and the GPS velocity analysis in Lebanon, Gomez et al. (2007) denied Butler et al. (1997) arguments and conclusions and proved historic and current tectonic and seismic activity of the northern segments of the Dead Sea transform fault in Syria and Lebanon. The sub-aerial flood basalts of the Early Miocene, mostly ranging in age from 20 to 16 Ma ago, spreaded over most of southern Syria, Jordan and Saudi Arabia, but were absent along the Syrian coastal zone (Mouty *et al.*, 1992). After a period of volcanic activity quiescence lasted till about 8 My ago an intensive volcanism commenced over most of Syria, but particularly along the northern and southern rims of the Northern Dead Sea Fault (Fig. 1). This phase of volcanism remained active into prehistoric time, for example, in the Karasu Valley, (Southern Turkey), in the northernmost part of the rift (Capan *et al.*, 1987) where ages range from 2 My to 0.4 My.

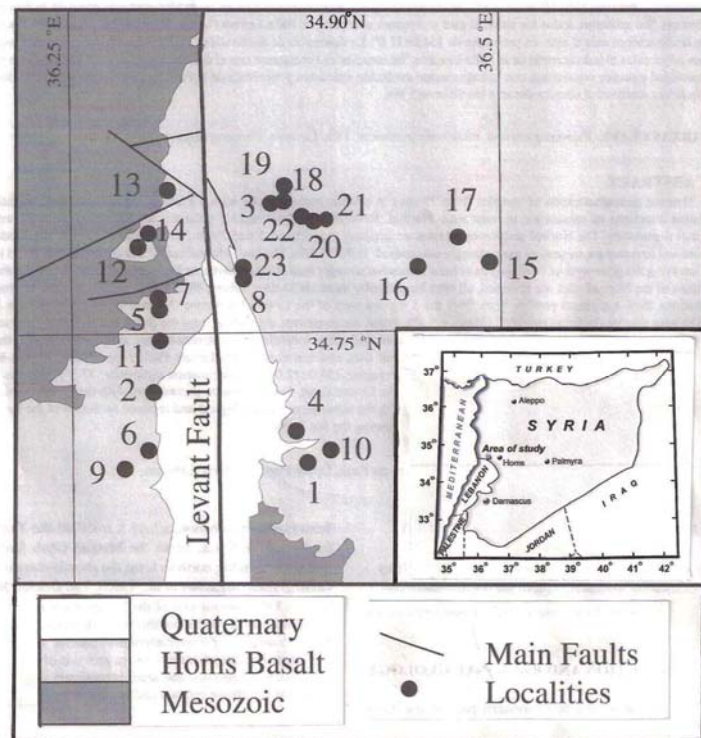


Figure 1. Outline geological map of the studied area.

The sampling localities represent mostly 3 sites per volcanic unit. The main N-S Northern Dead Sea Fault system (Levant Fault) is labelled in the figure, but, for clarity, the orientations of only a few relevant faults are marked. The fault trends are mainly N-S, NW-SE and NE-SW directions but only the main faults systems can be shown. Numbers are as follows:

1=T1-T3, 2=T4-T8, 3=T9-T12, 4=T13-T18, 5=T19-T21, 6=T22-T24, 7=T25-T27, 8=T28-T30, 9=T31-T33, 10=T34-T36, 11=T37-T39, 12=T40-T42, 13=T43-T45, 14=T46-T48, 15=T49-T51, 16=T52-T54, 17=T55-T57, 18=T58-T60, 19=T61-T63, 20=T64-T66, 21=T67-T69, 22=T70-T72, 23=T73-T75.

The studied area is mainly covered with the Upper Pliocene basaltic flows (βN^b_2) and the Quaternary sequences which are mostly consolidated sediments and are dominated by those of the Al Buqeiya depression. The area is divided by the main N-S extending Northern Dead Sea Fault and many other faults, which are mainly trending N-S, NW-SE and NE-SW, but only the main faults are shown in Figure 1.

The present research aimed to study the palaeomagnetism of the Upper Pleocene basaltic rocks from the western and eastern flanks of the Northern Dead Sea Fault system in the Buqeiya area NE of Tel Kalakh. 75 sites were sampled, each comprising 6-7 samples, in the Upper Pliocene (βN^b_2) basaltic flows, from the western flank and from the near and distant eastern flank of the Northern Dead Sea Fault. Generally, three sites were taken at separate locations within similar or identical exposures.

Sampling, Measurement and Treatment

Conventional palaeomagnetic drilling techniques (Collinson, 1983; Tarling, 1983) were employed by using petrol driven drill and sun compass was used for orientation. Then cores, 2.5 cm in diameter and 2.1 cm in height, were sliced to be measured by the magnetometer and demagnetizing instruments (Molyneux, 1971, Abou-Deeb, 1997 and Abou-Deeb *et al.*, 1999) in the Palaeomagnetic Laboratory of Plymouth University-England. The low-field susceptibility was measured after each magnetic intensity measurement. Representative samples from each of the main localities, were treated at 100, 150, 200, 250, 300, 350, 400, 450, 500, 520, 540, 560 & 580°C. Sample characteristic directions were defined where the vectors isolated had a mean angular deviation (*MAD*) of $< 5^\circ$ (Kirschvink, 1980). A site mean direction was considered further if it was defined by at least 5 samples with characteristic directions that agreed with an estimated 95% Probability cone of confidence of $< 15^\circ$ (Fisher, 1953), that is the

cone angle which is characterized by 95% probability that the true direction is located inside the cone is less than 15° . According to the study of the behavior of the pilot samples the rest of the samples were thermally demagnetized at 200, 300, 350, 400, & 420 °C. Apart from the strongly magnetized T56 site (intensity 116.5 A/m) (Table 1), the initial intensity of magnetization ranged from 31.4 A/m (site T44) to 0.59 A/m (site T66) with an average of 6.3 ± 6.4 A/m. The site low-field susceptibilities ranged from 3.4 mSI (T66) to 71.1 mSI (T22) with an average of 31.8 ± 17.1 mSI.

The magnetic susceptibility and intensity of magnetization of the pilot sample were studied in order to determine if any thermo-chemical changes had occurred to the magnetic minerals during heating. This will help in the extrapolation of the magnetic mineral that carries the magnetization of the rocks.

Results and Interpretations:

In the majority of sites, the samples had well defined characteristic directions during thermal demagnetisation, with their mean diagonal angles (*mda*) (Kirshvink, 1980) mostly being less than 3° . The main exceptions were in 5 sites (T4, T8, T13, T15, T59) in which most sample *mda*'s exceeded 5° ; these sites were excluded from further directional analyses. In the remaining sites (Abou-Deeb, 2004), the blocking temperature spectra suggested that the characteristic magnetic directions were carried by magnetite. Above about 350°C , the low field susceptibility tended to increase, but with no apparent effect on the linearity of the vector until approaching the Curie point of magnetite. In almost all samples, the temperature range within which a single vector was defined extended from $150\text{-}200^\circ$ to at least 400°C (Abou-Deeb & Tarling, 2005). A well defined site mean direction was isolated in most remaining sites, with the site mean estimate of precision, α_{95} (Fisher, 1953), being $<15^\circ$ (Table 1). However, 2 sites were rejected (T40 & T58) in which the precision estimate exceeded 15° and a further 2 sites (T9 & T10) because the number of acceptable sample directions became <5 .

As expected for the Late Pliocene, both Normal (N) and Reversed (R) polarities were present. Using the standard definitions (N = site virtual geomagnetic pole [VGP] latitude $>50^\circ\text{N}$; Reversed VGP $>50^\circ\text{S}$; Intermediate = site VGP between 50°N and 50°S), the majority of the sites, 41 were of Reversed polarity, 12 were of Normal polarity and 16 were of Intermediate polarity. The arithmetic mean site initial intensity of magnetisation of the Reversed polarity sites (5.18 ± 3.9 A/m) was

similar to that of the 12 Normally magnetised sites (6.74 ± 8.4 A/m). The 16 sites of Intermediate polarity sites were more strongly magnetised and much more scattered (18.4 ± 27.7 A/m) and still remained more strongly magnetic, but of similar scatter (11.9 ± 9.5 A/m) after removal of the most strongly magnetised site (T56). The 6 sites with scattered sample directions were also marginally more strongly magnetised (8.4 ± 7.4 A/m) than those of Normal or Reversed polarity although their scatter became similar. In contrast, the low-field susceptibility site arithmetic mean values were similar, irrespective of polarity; Reversed (29.5 ± 17.3 mSI), Normal (34.4 ± 12.1 mSI), Intermediate (31.1 ± 13.1 mSI) and Scattered (32.3 ± 12.5 mSI).

For tectonic interpretations (Abou-Deeb & Tarling, 2005), it is desirable to reduce any geomagnetic secular variation or non-axial dipole effects from the observed directions of remanence. On this basis, all 16 sites of Intermediate polarity were ignored and the polarity of the Normal sites were reversed by 180° so that all remaining 53 mean site vectors were southerly and of negative inclination (191.3° , -48.2° , $\alpha_{95}=2.7^\circ$). However, of these sites, there are some that show greater divergence from the overall mean direction than others, particularly in inclination. Assuming that tectonic rotations related to a major transform fault system would be largely about vertical axes, 11 site mean directions were initially rejected as having inclinations more than 8° (solid angle) from the mean inclination. The remaining 42 sites showed two clear declination populations – one SSW (between 182 - 195°) and the other SSE (between 146 - 167°). When plotted (Fig. 2) these populations showed a distinct local distribution. All SSW declinations are confined to the three regions west of the main Northern Dead Sea Fault (Marmarita, Qalat El-Hossen & Tel Kalakh 185.9° , -49.0° , $\alpha_{95}=3.6^\circ$) and the two regions more than *c.* 5 km east of the Fault (E. Ain-Kut & Sufer 197.5° , -46.8° , $\alpha_{95}=2.6^\circ$). These had a combined mean direction of 191.3° , -48.2° ($\alpha_{95} = 2.7^\circ$). Such a direction is consistent with that predicted for this part of the Arabian plate some 10 Ma, 185.6° , -49.9° , i.e. after allowing for the opening of the Red Sea and using the African polar wander path (Besse & Courtillot, 1991). This implies that such regions belong to the stable part of the Arabian Plate. In contrast, the sites in the eastern regions close to the Northern Dead Sea Fault (Bahur, W. Ain-Kut, Mzeineh & Buqeia) all have SSE site mean declinations, with a mean direction of 153.8° , -47.6° ($\alpha_{95} = 3.9^\circ$). This direction differs significantly in declination, by 37.7° , but is identical in inclination, suggesting that these sites are from areas that have been rotated anticlockwise, relative to stable Arabia, since they were formed some 5-6 Ma with Homs basalt.

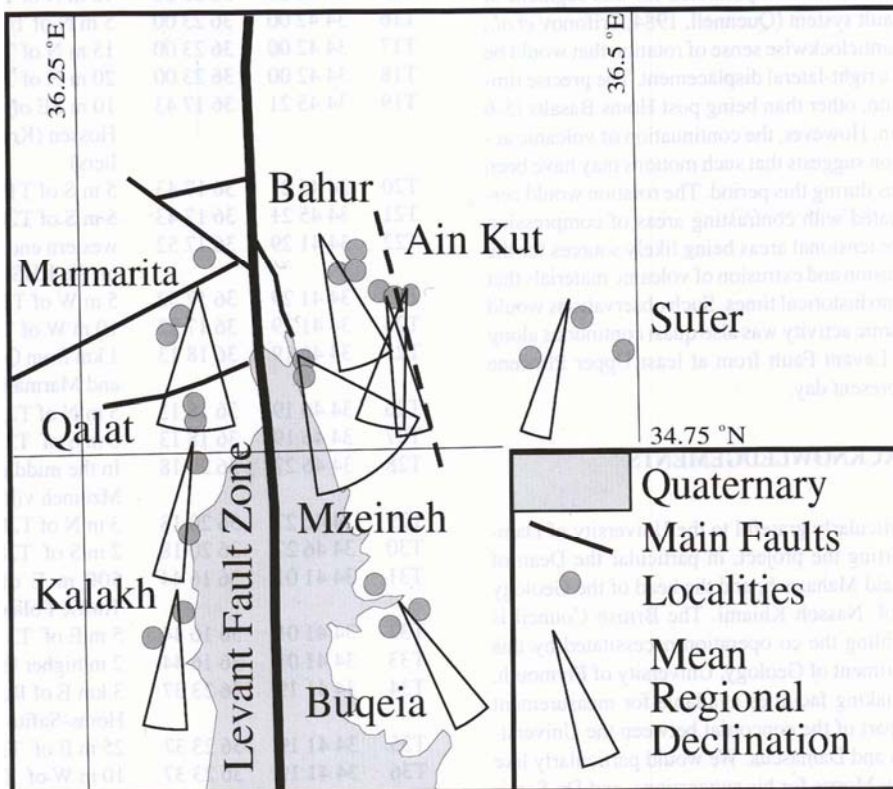


Fig. 2. The pattern of Mean Regional Declination. The circles, unlabelled, are the same locations as in Figure 1. The “pie wedge” are centered on the mean declination for each region, as listed in Table 1 and after inverting Normal polarities to Reversed, with the angle subtended by the wedge being based on error in declination $\pm\delta Dec.$, using the regional estimate of precision, α_{95} , given in Table 2.

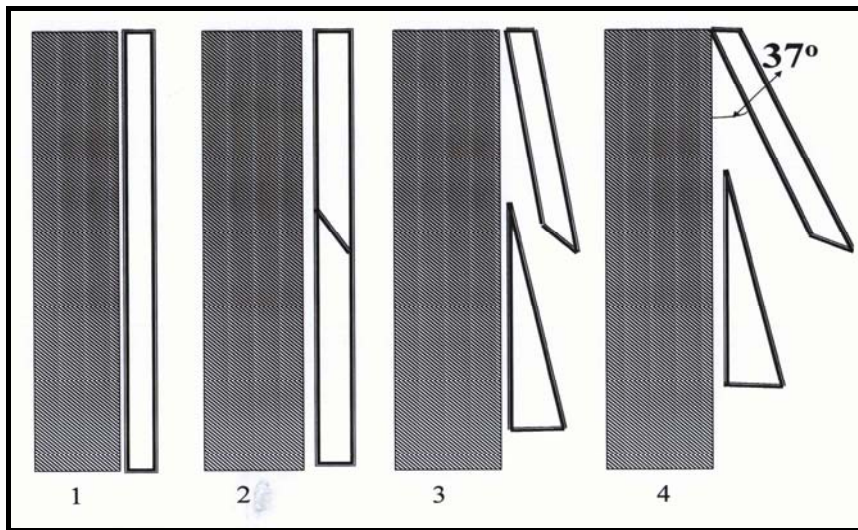
This 37.7° direction difference in declination is similar to the 37.0° angle that bisect the basaltic rocks on both sides of Al Buqeia. In order to explain the similarity between these two angles it is suggested that the rocks of the near eastern flank of Al Buqeia was rotated anticlockwise leading to the creation of Al Buqeia depression.

The western edge of this block is clearly the main Northern Dead Sea Fault itself, but the eastern flank is only defined in this study by the deep Al-Mnshar Valley, oriented N-S, that separates the sites in East and West Ain-Kut. The apparent rotation of these eastern tectonic

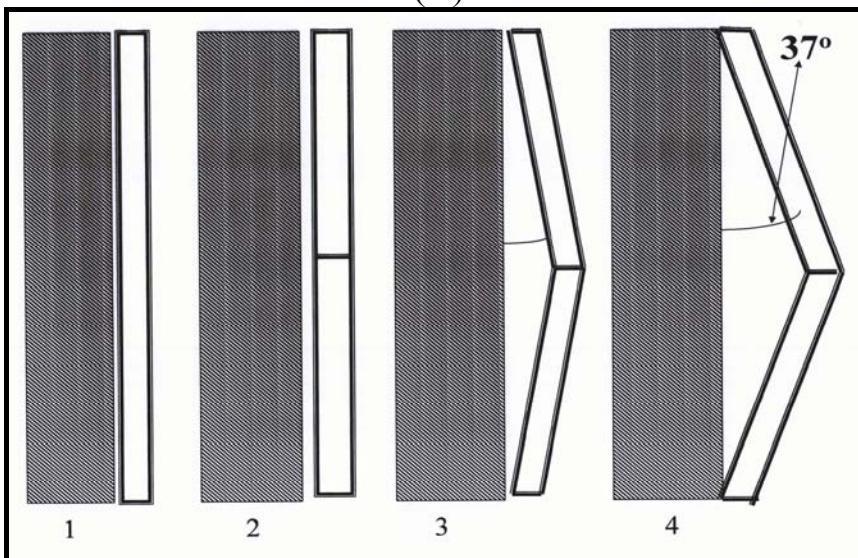
units within some 5 km of the main fault complex was unexpected by the author. It had originally been considered that far smaller units, possibly confined within the fault zone, may have shown evidence of the activity, or not, along this part of the Northern Dead Sea Fault system. The observed amount of dislocation is consistent with the 20-25 km of differential motion predicted for this segment of the Dead Sea Fault system (Quennell, 1984; Trifonov *et al.*, 1991), as is the anticlockwise sense of rotation that would be associated with a left-lateral displacement. The precise timing of the rotation, other than being post Homs Basalts (5-6 Ma), is uncertain. However, the continuation of volcanic activity in the region suggests that such motions may have been quasi-continuous during this period. The rotation would certainly be associated with contrasting areas of compression and tension – the tensional areas being likely sources for the intermittent intrusion and extrusion of volcanic materials that has continued into historical times. Such observations would only be consistent with seismic activity being quasi continuous along this part of the Northern Dead Sea Fault system from at least Upper Pliocene times until the present day.

The suggested scenario of rotation is as follows: at some time during the northward movement of the eastern flank of the Northern Dead Sea Fault, the movement, for some reason, blocked at the end of Al Buqeia depression, while the northward movement of the eastern flank is still going on, which forced the rocks of the Near Eastern Flank to rotate gradually with the southern part of this flank moving northward according to one of the mechanisms shown in Figure 3. If this had happened and if we accept that the length of this rotating Near Eastern Flank is 20 km then a possible shortening equal to 5 km, ($=20 \cdot \tan 37^\circ = 5 \text{ km}$).

This suggestion need to be proved from other branches of geology and geophysics.



(A)



(B)

Fig. 3. A and B are the two suggested scenarios of rotation in four steps. The black rectangles represent the stable western flank of Al-Buqeia and white rectangles represent the moving eastern flank of Al-Buqeia.

Table 1. Site Mean Intensity, Susceptibility, Direction of Remanence and pole position. The number of samples per site, with a vector defined with a mean angular deviation (*mda*) less than 5° (Kirshvink, 1980), is N compared with the total number of samples collected, n. The mean initial intensity of magnetization (Init. Int.) is in units of A/m and the mean susceptibility (Susc.) are in mSI units. The site mean directions (Declination, Decl. and Inclination, Incl.) are listed with the estimates of precision, *k*, and 95% Probability, α_{95} (Fisher, 1953). The polarity (Pol.) of each site is Normal (N), when the virtual geomagnetic pole latitude is greater than 50°N, Reversed (R), when greater than 50°S, and Intermediate (I) when between these two limits. "Scattered" sites (S) are when there are fewer than 5 samples with *MAD* < 5° or when the site precision, α_{95} , exceeds 15°.

Site		Init. Int.	Susc.	Direction				Polarity
	N/n	(A/m)	(mSI)	Decl.	Incl.	<i>k</i>	α_{95}	Pol.

Western flank

Marmarita

T40	5/6	7.4±1.1	36.6±2.3	scattered		21	17.0	S
T41	5/6	5.3±0.2	8.6±1.9	112.7	-62.2	1671	1.9	I
T42	6/6	2.2±0.8	6.8±1.1	170.5	-66.9	134	5.8	R
T43	6/6	21.5±3.3	30.9±1.5	73.9	4.3	161	5.3	I
T44	6/6	31.4±4.9	28.1±1.0	57.4	5.4	423	3.3	I
T45	6/6	12.2±1.47	21.9±3.6	33.4	16.3	300	3.9	I
T46 ^{pd}	5/6	1.86±0.45	63.4±2.1	175.8	-54.1	165	6.0	R
T47 ^{pd}	5/6	2.27±0.26	49.7±1.5	182.5	-43.1	318	4.3	R
T48 ^{pd}	6/6	1.87±0.17	53.6±2.2	185.4	-42.4	483	3.1	R

Qalat El-Hossen

T19	6/6	5.2±0.3	21.2±1.7	195.5	-49.2	944	2.2	R
T20	5/6	3.0±0.1	6.8±0.7	189.9	-49.9	1319	2.1	R
T21	6/6	3.1±0.1	10.6±2.0	187.7	-48.1	1375	1.8	R
T25	4/7	4.7±1.4	38.0±3.5	132.1	-18.3	43	14.2	I
T26	6/6	4.4±0.6	44.1±3.0	131.0	-13.2	308	3.8	I
T27	6/6	2.9±0.9	32.1±1.3	145.0	-24.1	178	5	R
T37	6/7	8.4±1.6	20.0±6.2	192.8	-32.5	162	4.8	R
T38	5/6	12.4±1.8	22.5±2.4	209.0	-7.7	54	10.5	R
T39	6/6	11.3±1.9	22.7±2.0	195.6	-21.2	240	4.5	R

Tel Kalakh

8.5±0.8 Ma

T4		2.8±0.5	32.4±1.0	undefined				S
T5	5/6	5.4±1.9	31.9±6.7	120.3	-59.9	121	152.3	I
T6	4/6	3.4±1.4	11.3±5.1	109.6	-56.1	175	150.4	I
T7	5/6	4.2±0.7	13.4±2.6	115.6	-54.7	231	146.6	I
T8		4.5±0.4	7.9±0.4	undefined				S
T22	6/6	2.7±0.4	71.1±3.0	175.8	-48.6	467	72.2	R
T23	6/6	4.0±1.5	57.2±11.0	177.5	-51.4	1057	75.8	R

T24	6/6	5.9±1.0	65.4±4.4	173.7	-49.6	1091	89.6	R
T31	6/6	3.8±0.3	30.2±2.2	190.9	-51.2	77	320.4	R
T32	7/7	3.9±1.0	33.5±1.8	197.5	-47.5	347	323.6	R
T33	7/7	5.5±1.2	31.7±0.8	198.2	-49.6	45	316.8	R

Eastern Flank

E. Ain-Kut 5.25±0.2; 5.08±0.16 Ma

T64	6/6	1.7±0.4	13.9±5.0	199.4	-43.1	1915	331.3	R
T65	6/6	1.0±0.1	6.2±0.4	199.0	-45.9	1760	325.9	R
T66	6/6	0.6±0.1	3.4±0.3	194.2	-50.2	727	320.4	R
T67	5/6	1.6±0.3	27.2±3.6	199.4	-51.6	574	309.9	R
T68	6/6	1.6±0.2	24.9±5.0	202.4	-40.8	108	330.8	R
T69	6/6	2.5±0.7	40.3±2.3	199.7	-44.9	440	327.2	R

W. Ain-Kut

T70 ^d	6/6	7.1±0.6	6.1±0.9	165.9	-47.8	1667	103.7	R
T71 ^d	6/6	8.5±1.1	10.6±1.0	163.0	-47.9	1556	109.1	R
T72 ^d	6/6	20.9±3.4	7.6±2.2	171.5	-41.3	1581	72.4	R

Bahur 6.2±0.2 Ma; 5.21±0.17 Ma; 5.08±0.16 Ma

T9	3/6	1.7±0.2	11.7±1.5	(175.4	-19.0)	124	47.0	R
T10	3/6	3.0±0.4	30.5±1.6	(156.82	-25.9)	207	86.8	R
T11	5/6	4.0±1.0	31.1±3.1	146.7	-40.5	136	113.4	R
T12	5/6	3.5±0.6	25.7±2.9	164.3	-46.7	86	103.4	R
T58	4/6	22.9±18.1	43.3±2.3	Highly scattered				S
T59	2/6	26.2±10.2	33.6±2.4	(294.0	-57.3)	575	262.7)	I
T60	4/6	3.9±0.2	34.3±1.0	19.6	56.8	195	111.6	N
T61 ^{pd}	6/6	3.9±0.2	38.7±1.2	343.2	53.7	163	308.8	N
T62 ^{pd}	6/6	3.6±0.2	57.5±3.1	338.2	55.3	380	316.1	N
T63 ^{pd}	6/6	2.9±0.2	36.8±2.4	347.6	45.8	321	274.1	N

Mzeineh

T28	4/6	4.4±2.4	17.0±2.5	0.4	48.4	127	212.6	N
T29	5/6	2.4±0.5	15.6±2.3	143.2	-37.8	158	113.3	R
T30	6/6	3.1±0.2	18.4±3.0	128.4	-27.3	161	116.1	I
T73	6/6	7.3±0.7	24.7±1.8	342.1	51.3	153	300.8	N
T74	4/6	5.4±0.4	27.9±1.5	342.7	72.0	40	13.8	N
T75	6/6	33.0±1.3	14.8±0.7	314.7	51.6	519	315.7	N

Sufer 4.85±0.15 Ma; 5.64±0.18

T49	6/6	3.9±0.4	33.5±2.0	18.1	46.9	618	2.7	N
T50	6/6	3.8±0.4	40.6±2.9	12.2	45.8	379	3.4	N
T51	6/6	3.1±0.3	47.9±1.8	12.2	46.5	643	2.6	N
T52	6/6	11.9±3.8	48.4±1.8	314.7	-1.7	659	2.6	I
T53	6/6	19.6±3.2	51.0±6.2	308.8	0.2	452	3.2	I
T54	5/6	20.2±1.0	39.8±1.7	254.7	-1.2	1126	2.3	I
T55	6/6	5.0±1.7	40.7±4.0	256.1	-8.0	112	6.4	I
T56	6/6	116.5±5.1	37.4±2.5	257.5	-17.5	325	3.7	I
T57	5/6	5.8±2.0	38.9±6.7	17.8	52.4	122	6.9	N

Buqeia 5.4±0.1 Ma

T1	7/7	7.0±0.9	40.1±2.5	144.8	-48.9	166	4.7	R
T2	5/6	5.2±0.6	43.1±3.3	141.9	-43.9	139	6.5	R
T3	6/6	6.3±1.0	40.8±2.6	151.3	-48.9	225	4.5	R
T13		8.6±1.3	34.8±2.4	undefined				S
T14	5/6	9.3±3.7	33.2±1.3	145.1	-46.9	164	7.2	R
T15		4.1±0.7	38.8±1.0	undefined				S
T16	6/6	4.5±2.8	30.9±0.7	167.7	-50.0	179	5.0	R
T17	6/6	5.65±0.4	41.1±2.2	166.5	-44.8	241	4.3	R
T18	6/6	9.5±0.5	36.0±1.3	147.4	-22.6	296	3.9	R
T34	6/6	7.6±0.8	29.5±1.5	136.1	-45.9	709	2.5	R
T35	6/7	6.5±3.6	41.2±4.0	151.4	-48.9	701	2.5	R
T36	6/6	10.9±4.3	22.4±1.8	134.5	-40.8	87	7.2	R

Table 2. The mean directions and parameters of the accepted sites in the western and eastern flanks of the Northern Dead Sea Fault. Symbols as in Table 1.

Locality	Sites	Decl.	Incl.	k	α_{95}	Site Numbers
Western Flank						
Marmarita	3	181.6	-46.6	122	11.2	T46-T48
Qalat El-Hossen	3	191.0	-49.1	843	4.3	T19-T21
Tel Kalakh	6	185.7	-50.1	119	6.2	T22-T24, T31-T33
Far Eastern Flank						
E. Ain-Kut	3	199.1	-46.1	321	3.7	T64-T69
Sufer	4	195.0	-47.9	464	4.3	T49-T51, T57
Near Eastern Flank						
W. Ain-Kut	3	167.0	-45.7	278	7.3	T70-T72
Bahur	5	159.7	-48.7	95	7.9	T11, T12, T61-T63
Mzeineh	3	146.4	-47.4	45	18.6	T29, T73, T75
Buqeia	9	148.5	-47.1	87	5.5	T1-T3, T14, T16, T17, T34-T36
Western Flank	12	185.9	-49.0	149	3.6	
Far Eastern Flank	10	197.5	-46.8	352	2.6	
“Stable” Zones	22	191.3	-48.2	138	2.7	
Rotated Zone	20	153.8	-47.6	71	3.9	
The possible rotation	191.3-153.8=37.5					

REFERENCES

- Abou-Deeb, J. M. (1997). Studies of some magnetic and physical properties of some Quaternary - Recent basaltic rocks (Jabal Al-Arab, Syria). *Damascus University Journal (Basic Sciences)*, Vol. 13, No. 1, pp. 131-151.
- Abou-Deeb, J. M., Otaki, M. M., Tarling, D. H. and Abdeldayem, A. L. (1999). A palaeomagnetic study of Syrian volcanic rocks of Miocene to Recent age. *Geofisica Internacional*, 38, (1) 17-26.
- Abou-Deeb, J. M. (2004). A new Upper Pliocene palaeomagnetic from Western Syria and a preliminary Polar Wander Curve of the Arabian Plate. (Republic of Yemen). *Damascus University Journal, (Basic Sciences)*, Vol. 20, No. 2, 31-58.
- Abou-Deeb, J. M. and Tarling, D. H. (2005). A palaeomagnetic study of Upper Pliocene volcanic rocks in the area of the Levant Fault near Homs, western Syria. *Geofisica Internacional*, Vol. 44, No. 3, pp. 221-230.
- Ambraseys, N. N. and Barazangi, M. (1989). The 1759 earthquake in the Bakaa Valley: implications for earthquake hazard assessment in the Eastern Mediterranean region. *Jour. Geophys. Res.* Vol. 94, No.B4, p. 4007-4013.
- Ben-Menahem, A., Nur, A. and Vered, M. (1976). Tectonics, seismicity and structure of the Afro-Eurasian junction- the breaking of an incoherent plate. *Phys. Earth Planet. Inter.*, Vol. 12, pp. 1-50.
- Besse, J. and Courtillot, V. (1991). Revised and synthetic apparent polar wander paths of the African, Eurasian, North American and Indian Plates, and true polar wander since 200 Ma. *J. Geophys. Res.*, 96, 4029-4050.
- Best, J., Barazangi, M., Al-Saad, D., Sawaf, T., and Gebran, A. (1993). Continental margin evolution of the northern Arabian platform in Syria. *Amer. Assoc. Petrol. Geol. Bull.*, 77, 173-193.
- Beydoun, Z. (1999). The Evolution and development of the Levant (Dead Sea Rift) Transform System: a historical-chronological review of a structural controversy, in "Continental Tectonics", pp. 239-255, eds MacNiocail, C. & Ryan, P.D., Geological Society of London, London.
- Brew, G., Lupa, J., Barazangi, M., Sawaf, T., Al-Imam, A. and Zaza, T. (2001). Structure and tectonic development of the Ghab basin and the Dead Sea fault system, Syria. *Jour. Geol. Soc.*, London, Vol. 158. p. 665-674.
- Butler, R. W. H., Spencer, S. and Griffith, H. M. (1997). Transcurrent fault activity on the Dead Sea Transform in Lebanon and its implications for plate tectonics and seismic hazard. *Jour. Geol. Soc.*, London, 154, 757-760.
- Capan, U. Z., Vidal, Ph., and Cantagrel, J. M. (1987). K-Ar, Nd, Sr and Pb isotopic study of Quaternary volcanism in Karasu valley (Hatay), N-end of the Dead Sea Rift zone in SE-Turkey. *Yerbilimleri*, 14, 165-178.
- Chaimov, Th., Barazangi, M., Al-Saad, D., Sawaf, T., and Gebran, A. (1990). Crustal shortening in the Palmyrides fold belt, Syria, and implication for movement along the Dead Sea Fault system. *Tectonics*, vol. 9, No. 6, 1369-1386.
- Chorowicz, D., Dhont, D., Ammar, O., Rukieh, M., and Bilal, A. (2005). Tectonics of Pliocene Homs basalts (Syria) and implications for the Dead Sea Fault Zone activity. *Jour. Geol. Soc.*, London, vol. 162, 259-271.

- Collinson, D.W. (1983). *Methods and Techniques in Rock Magnetism and Palaeomagnetism*, Chapman & Hall, London, pp.503.
- Dubertret, L. (1970). Review of the structural geology of Red Sea and surrounding areas; Royal Society of London Philosophical Transaction, ser. A, 267, 9-20.
- Fisher, R. A. (1953). Dispersion on a sphere. *Proc. Roy. Soc.*, p A217, 295-305.
- Freund, R., Zak, I., Goldberg, M., Weissbrod, T. and Derin, B. (1970). The shear along the Dead Sea rift, *Philos. Trans. R Soc. London. Vol. A267*, 107-130.
- Garfunkel, Z., Zak, I., and Freund, R. (1981). Active faulting in the Dead Sea rift. *Tectonophysics*, 80, 1-26.
- Girdler, R. W. (1990). The Dead Sea transform fault system. *Tectonophysics*, 180, 1-13.
- Gomez, F., Meghraoui, M., Darkal, A. N., Hijazi, F., Mouty, M., Suleiman, Y., Sbeinati, R., Darawcheh, R., and Barazangi, M. (2003). Holocene faulting and earthquake recurrence along the Serghaya branch of the Dead Sea fault System in Syria and Lebanon. *Geophys. Jour. Int.*, 153, 658-674.
- Gomez, F., Khawlie, M., Tabet, C., Darkel, A.N., Khair, K., and Barazangi, M. (2006). Late Cenozoic uplift along the northern Dead Sea transform in Lebanon and Syria. *Earth Planet. Sci. Lett.*, 241, 913-931.
- Gomez, F., Karam, G., Khawlie, M., McClusky, S., Vernant, P., Reilinger, R., Jaafar, R., Tabet, C., Khair, K., and Barazangi, M. (2007). Global positioning System measurements of strain accumulation and slip transfer through the restraining bend along the Dead Sea fault System in Lebanon. *Geophys. Jour. Int.* 168, 1021-1028.
- Hempton, M. (1987). Constraints on Arabian plate motion and extensional history of the Red Sea. *Tectonics*, 6, no.6, p 687-705.
- Jestin, F., Huchon, P. and Gaulier, J.M. (1994). The Somalia plate and the Eastern African Rift system, present-day kinematics, *Geophysics Jou. Int.*, 116, p 637-654.
- Joffe, S. and Garfunkel, Z. (1987). Plate kinematics of the circum Red Sea – a re-evaluation. *Tectonophysics*, 141, 5-22.
- Kellogg, K. S. and Rynolds, R. L. (1983). Opening of the Red Sea: constraints from a palaeomagnetic study of the As Sarat volcanic field, south- western Saudi Arabia. *Geophys. J. Roy. Astro. Soc.*, 74, 649-665.
- Khair, K., Khawlie, M., Hadda, F., Barazangi, M., Seber, D. and Chaimov, T. (1993). Bouguer gravity and crustal structure of the Dead Sea transform fault and adjacent mountain belts in Lebanon. *Geology*, Vol. 21, p. 739-742.
- Kirschvink, J. L. (1980). The least-squares line and plane and the analysis of palaeomagnetic data. *Geophys. J. R. astr. Soc.*, 62, 699-718.
- Meghraoui, M., Gomez, F., Sbeinati, R., Woerd, J. V., Mouty, M., Darkal, A. N., Radwan, Y., Layyous, I., Al Najjar, H., Darawcheh, R., Hijazi, F., Al-Ghazzi, R., and Barazangi, M. the Dead Sea Rift (2003). Evidence for 830 years of seismic quiescence from palaeoseismology, archaeoseismology and historical seismicity along the Dead Sea Rift in Syria. *Earth Planet. Sci. Lett.*, 210, 35-52.

- Menzies, M. A., Bosence, D. W. J., El-Nakhal, H. A., Al-Khirbash, S., Al-Kadasi, M. A. and Al-Subbary, A. K. (1990). Lithospheric extension and the opening of the Red Sea: sediment-basalt relationship in Yemen. *Terra Nova*, 2, 340-350.
- Molyneux, L.M. (1971). A complete results magnetometer for measuring the remnant magnetization of rocks. *Geophys. J. R. astr. Soc.*, 24, 429-433.
- Mouty, M., Delaloye, M., Fontignie, D., Piskin, O., and Wagner, J. (1992). The volcanic activity in Syria and Lebanon between Jurassic and the Actual. *Schweiz. Mineral. Petrogr. Mitt.*, 72, 91-105.
- Ponikarov, V. P. (1966). (Editor). Explanatory notes on the Geological Map of Syria: Scale 1:1,000,000, Ministry of Industry, Damascus, Syria.
- Quennell, A. M. (1984). The Western Arabian rift system. In: Dixon, J.E. & Robertson, A. H. F. (eds.) *The Geological Evolution of the Eastern Mediterranean*. Geological Society, London. Special Publication, 17, 775-788.
- Ron, H. (1987). Deformation along the Yemmunah, the restraining bend of the Dead Sea transform, palaeomagnetic data and kinematic implication. *Tectonics*, 6, 653-666.
- Sigachev, S. P., Kopp, M. I., Elias, K., Hafez, A., Adzhamyanyan, Z.H., and Fakyani, F. (1995). Tectonic data for the Levant fault by using mesotectonic measures (Ghab and Missyaf areas). *Geological Sciences Review*, Damascus, 5, 75-81, (In Arabic).
- Tarling, D. H. (1983). *Palaeomagnetism*, Chapman & Hall, London, pp.379.
- Trifonov, V.G., Trubikhin, V.M., Adzhamyanyan, Z., Dzhallad, S., El-Khair, Y. and Ayed, K. (1991). Levant fault zone in northwest Syria. *Geotectonics*, 25, 145-154.
- Walley, C. D. (1988). A braided strike-slip model for the northern continuation of the Dead Sea fault and its implications for Levantine tectonics. *Tectonophysics*, 145, 63-72.